https://doi.org/10.5194/os-2019-122
Preprint. Discussion started: 11 December 2019

Ocean Science Discussions
Open Access

A monthly tidal envelope classification approach for semi-diurnal regimes with variability in S_2 and N_2 tidal amplitude ratios

Do-Seong Byun[1], Deirdre E. Hart[2]

[1]Ocean Research Division, Korea Hydrographic and Oceanographic Agency, Busan 49111, Republic of Korea
[2]School of Earth and Environment, University of Canterbury, Christchurch 8140, Aotearoa New Zealand

Correspondence to: Deirdre E. Hart (deirdre.hart@canterbury.ac.nz)

Abstract. In a world of increasing coastal inundation hazards, an understanding of daily through to monthly tidal envelope characteristics is fundamental to resilient coastal management and development practices. For decades, scientists have described and compared daily tidal forms around the world's coasts based on the four main tidal amplitudes. Our paper builds on this 'daily' method by adjusting the constituent analysis to distinguish the different monthly types of tidal envelope occurring in the semi-diurnal coastal waters around Aotearoa New Zealand. Analyses of tidal records from 23 stations are used, alongside data from the FES2014 tide model database and theoretical experiments, in order to find the key characteristics and constituent ratios of tides that can be used to classify monthly tidal envelopes. The resulting monthly tidal envelope classification approach described (F_M^S) is simple, complementary to the successful and much used daily tidal form factor (F), and of use for coastal flooding, climate change and maritime operation management and planning applications in semi-diurnal regimes.

1 Introduction

Successful human-coast interactions in the world's low-lying areas are predicated upon understanding the temporal and spatial variability of sea levels (Cartwright, 1999; D'Onofrio et al., 1999; Nicholls et al., 2007). This is particularly the case in island nations like Aotearoa New Zealand (ANZ), where over 70% of the population reside in coastal settlements (Stephens 2015). An understanding of tidal water level variations is fundamental to resilient inundation management and coastal development practices in such places (Masselink et al., 2014; Olson, 2012; Pugh, 1996), as well as to accurately resolving non-tidal signals of global interest, such as in studies of sea level change and gravimetry (Egbert et al., 1994; Stammer et al., 2014).

In terms of daily cycles, tidal form factors or form numbers (F) based on the amplitudes of the four main tidal constituents (K_1, O_1, M_2, S_2) have been successfully used to classify tidal observations from the world's coasts into four types of tidal regime for nearly a century (Figure 1 a). Originally developed by van der Stok (1897), with a fourth category added by Courtier (1938), these simple and useful form factors comprise the ratio between the combined K_1 and O_1 diurnal amplitudes versus the combined M_2 and S_2 semi-diurnal amplitudes (Table 1). The resulting form factors classify tidal regimes into those which roughly experience one high and one low tide per day (diurnal regimes); or two approximately equivalent high and low tides per day (semidiurnal regimes); or two unequal high and low tides per day (mixed semidiurnal dominant or mixed diurnal dominant regimes) (e.g. Defant 1958).

Albeit not part of their original design, some interpretation of the tidal envelope types observed at fortnightly and monthly timescales has accompanied use of daily tidal form classifications (e.g. Pugh, 1996; Pugh & Woodworth, 2014). Whereas the daily tidal form factor identifies the number and form (equal or mixed) of tidal height cycles typical within a lunar day (i.e. 24 hours and 48 minutes) at a particular site, a tidal envelope describes the maximum and minimum boundaries of tidal height cycles occurring across a specified timescale at that site. The envelope timescale of interest in this paper is monthly.

Tidal envelopes at monthly scales depend on tidal regime. In general, semi-diurnal tidal regimes often feature two spring-neap tidal cycles per synodic (lunar) month (Table 1). These two spring-neap tidal cycles are usually of unequal magnitude, due to the effect of the moon's perigee and apogee, which cycle over the period of the anomalistic month. In contrast, diurnal tidal regimes exhibit two pseudo spring-neap tides per sidereal month. For semi-diurnal regions where the N_2 constituent contributes significantly to tidal ranges, tidal envelope classification should consider relationships between the M_2, S_2, and N_2 amplitudes. The waters around ANZ represent one such region: here the daily tidal form is consistently semi-diurnal, but large differences occur between sites within this region in terms of their typical tidal envelope types over fortnightly to monthly timescales.

The primacy placed on the four main amplitudes used in daily tidal form calculations has influenced the constituents examined in comparisons between global tide models and satellite altimeter data (e.g. Andersen, 1995; Stammer et al., 2014), emphasizing the importance of daily and spring-neap constituents. Far less attention has been paid to of the importance of other constituents in modern tidal research. More than eighty years after the development of the ever-useful daily tidal form factors, attention to the regional distinction between different tidal envelope types within the semi-diurnal category is also needed, and forms the motivation for this paper. In this first explicit attempt to classify monthly tidal envelope types, we examined the waters around ANZ, a strong semi-diurnal regime with relatively weak diurnal tides (daily form factor F <0.15) and variation in the importance of the S_2 and N_2 amplitude ratios. The result is an approach for classifying monthly tidal envelope types that is transferable to any semi-diurnal regime. As well as providing greater understanding of the tidal regimes of ANZ, we hope that our paper opens the door for new international interest in classifying tidal envelope variability at multiple timescales, work which would have direct coastal and maritime management application including contributing to explanations of the processes behind delta city coastal flooding hazards and their regional spatial variability.

2 Methodology

2.1 Study area

Aotearoa New Zealand is a long (1600 km), narrow (≤400 km) country situated in the south-western Pacific Ocean and straddling the boundary between the Indo-Australian and Pacific plates. Its three main islands, Te Ika-a-Māui or the North Island, Te Wai Pounamu or the South Island, and Rakiura or Stewart Island, span a latitudinal gradient between about 34° and 47° South. The tidal regimes in the surrounding coastal waters are semi-diurnal, with variable diurnal inequalities, and absolute tides that span micro through to macro tidal ranges. Classic spring-neap cycles are present in western areas of ANZ, while eastern areas feature distinct perigean-apogean influences (Byun and Hart, 2015; Heath, 1977, 1985; LINZ, 2017b; Walters et al., 2001).

Highly complex tidal propagation patterns occur around ANZ, including a complete semi-diurnal tide rotation: contrary to the southern hemisphere Coriolis Effect, the tide generally circulates around this country in an anti-clockwise direction. This occurs due to the forcing of M_2 and N_2 tides by two amphidromes, situated northwest and southeast of the country, producing trapped Kelvin waves; while the S_2 and K_1 tides exhibit a single wave front generated by an amphidrome to the southeast, plus refraction of a trapped wave around the South Island. Around Te Moana-o-Raukawa or Cook Strait, the waterway between the two main islands, tides travelling north along the east coast run parallel to tides travelling south along the west coast. The pronounced differences between these east/west tidal states, combined with their tidal range differences, together produce marked differences in amplitude and strong current flows through Cook Strait (Heath, 1985; Walters et al., 2001, 2010).

2.2 Data analysis approach

Year-long sea level records were sourced from a total of 23 stations spread around ANZ (Figure 2): eighteen 1 minute-interval records from Land Information New Zealand (LINZ, 2017a); and five 1 hour-interval records from the National Institute of Water and Atmospheric Research (NIWA, 2017). For both the LINZ and NIWA data, years with good quality hourly data

https://doi.org/10.5194/os-2019-122
Preprint. Discussion started: 11 December 2019

were selected for analysis from amongst multi-year records. The 23 tidal records were harmonically analyzed using T_Tide (Pawlowicz et al., 2002) to examine spatial variation in the main tidal constituents' amplitudes, phase-lags, and amplitude ratios, between regions and in comparison with their tidal potential values from Equilibrium Theory (see Table A1 for raw results). An additional set of tidal constituent amplitude data was sourced from Tables 1 and 3 of Walters et al. (2010), derived from 33 records of between 14 and 1900 days length, from around the greater Cook Strait area between ANZ's two main islands, where spring-neap tides reach the strongest in the country.

We then classified the monthly tidal envelope types found around ANZ based on detailed examination of constituent ratios produced from the tidal harmonic analysis results, as well as data from the FES2014 tide model (see Carrere et al., 2016 for a full description of this database), and experimental plots of the different tidal envelope types generated from this constituent data. Due to the strong semi-diurnal tidal regimes in the study area, and similar to the approach of Walters et al. (2010), we were able to ignore sidereal (K_1, O_1) effects and simply consider the effects of spring-neap (M_2, S_2) and perigean-apogean cycles (M_2, N_2) in our monthly tidal envelope type characterization.

3 Results

3.1 Key tidal constituent amplitudes and amplitude ratios

In order to better understand the key constituents responsible for shaping tidal height forms around ANZ, we first mapped variability in the amplitudes of the semi-diurnal and diurnal constituents listed in Table 1 (Figure 3) and of the ratio values of the semi-diurnal constituent amplitudes (Figure 4). Table 2 summarizes these data, and contrasts them with those from Defant's (1958) Equilibrium Theory, while Table A1 catalogues the detailed data results.

Tidal amplitude ratio comparisons confirmed that the waters around ANZ are dominated by the three astronomical semi-diurnal tides: M_2, S_2 and N_2 (Table 2), the combination of which can generate fortnightly spring-neap tides (M_2 and S_2) and monthly perigean-apogean tides (M_2 and N_2). Figure 3 reinforces the relatively minor magnitudes of diurnal constituent amplitudes (O_1, K_1), as well as revealing the stronger west coast amplitudes of the spring-neap cycle generating constituents (M_2 and S_2), the relatively weak S_2 amplitudes overall (half that of Equilibrium Theory), and the more concentric pattern around ANZ of the perigean-apogean cycle generating N_2 amplitude.

In terms of the semi-diurnal constituent amplitude ratios, Figure 4 and Table 2 show that $\frac{a_{S_2}}{a_{M_2}}$ values cover a broad range around ANZ (0.04 to 0.47), with most sites exhibiting relatively smaller values (<0.27 at 22 out of 23 sites) than that of Equilibrium Theory (0.466). In contrast, $\frac{a_{N_2}}{a_{M_2}}$ ratios were found to be more stable around ANZ (values ranging from 0.16 to 0.23) and similar in magnitude to Equilibrium Theory (i.e. 0.191). By grouping the constituent amplitude and amplitude ratio results (Figures 3 to 4), we were able to distinguish four distinct monthly tidal envelope regimes around ANZ (Table 2).

- Firstly, '*spring-neap*' type tidal regimes occur where the S_2 tide amplitude is large compared to that of the N_2 (Table 2, Figure 3). In these areas there are two spring-neap tides per month with similar ranges, and negligible influence of perigean-apogean cycles. Such a regime occurs in the Kapiti and Cook Strait area (Figure 1), where the N_2 and M_2 amplitudes reduce by 75 to 90%, but the S_2 amplitude reduces by only about 30%, compared to on adjacent coasts.

- In direct contrast, there are '*perigean-apogean*' type tidal regimes, in areas where the N_2 amplitude strongly dominates over the S_2 (Table 2, Figure 3). In this type of tidal regime, the M_2 and the N_2 tides combine to produce strong signals over anomalistic timeframes (27.5546 days). Hence the highest tidal ranges in any given month occur in relation to the perigee, when the moon's orbit brings it close to Earth, rather than in line with the moon's phase, as is typical in spring-neap regimes. This type of regime occurs, for example, around the northern Chatham Rise near Kaikoura, and as far north as Castle Point on the east coast of the South Island.

https://doi.org/10.5194/os-2019-122
Preprint. Discussion started: 11 December 2019

The remaining coastal waters around ANZ can be separated into two tidal sub-regions, one with strong spring-neap signals and the other with strong perigean-apogean signals, but both with overall mixed or *intermediate* monthly tidal envelope types (Table 2). We distinguished these two envelope types via the combined variability of the ratios of $\frac{a_{\mathrm{S}_2}}{a_{\mathrm{M}_2}}$ and $\frac{a_{\mathrm{N}_2}}{a_{\mathrm{M}_2}}$ (i.e. of the spring-neap cycle; and perigean-apogean cycle forming tides, respectively). By examining these ratios we take account of the moderating influence of the M_2 tide at both synodic and anomalistic timeframes. In brief, the $\frac{a_{\mathrm{S}_2}}{a_{\mathrm{M}_2}}$ and $\frac{a_{\mathrm{S}_2}}{a_{\mathrm{N}_2}}$ ratios vary widely around ANZ, with highest values in the west, lowest values in the east, and intermediate values to the north and south (Figure 4). By comparison, $\frac{a_{\mathrm{N}_2}}{a_{\mathrm{M}_2}}$ values are relatively stable and high, except in a relatively small area of central Cook Strait, where this ratio drops and thus spring-neap cycles predominate (see 'spring-neap' type regimes above). The combined variability in these two ratios means that, except where we find 'perigean-apogean' or 'spring-neap' type monthly tidal envelope types, spring-neap tides do occur but the overall monthly envelope shape is fundamentally altered (asymmetrically) due to the perigean-apogean influence.

- In the first of the 'intermediate' monthly envelope sub-regions, tides exhibit two dominant, but unequal, spring-neap cycles per month due to a subordinate, but still influential, perigean-apogean effect. We term this type of monthly tidal envelope an '*intermediate, predominantly spring-neap*' type regime. Here values of $\frac{a_{\mathrm{S}_2}}{a_{\mathrm{N}_2}}$ are ≥1, with S_2 amplitudes reaching only around 17 to 50% those of the M_2 constituent (Figures 3 to 4; Table 2). Also in these areas, values of $\frac{a_{\mathrm{S}_2}+a_{\mathrm{N}_2}}{a_{\mathrm{M}_2}}$ are ≥0.45. This type of tide occurs, for example, at the Westport and Puysegur sites.

- In the other 'intermediate' monthly envelope sub-region, tides exhibit a mainly perigean-apogean form with a weaker, but noticeable, spring-neap signal: we term this envelope type as '*intermediate, predominantly perigean-apogean'*. Here values of $\frac{a_{\mathrm{S}_2}}{a_{\mathrm{N}_2}}$ sit between 0.3 and <1, while values of $\frac{a_{\mathrm{S}_2}+a_{\mathrm{N}_2}}{a_{\mathrm{M}_2}}$ are 0.3 to 0.4 (Figure 4, Table 2). This type of tide occurs, for example, at the Auckland and Sumner sites.

Figure 5 illustrates the four types of monthly tidal envelope found around ANZ as idealized types, two with stronger spring-neap signals (hereafter referred to as Types 1 and 2, see Figure 5 a-b) and two with stronger fortnightly perigean-apogean signals (hereafter Types 3 and 4, see Figure 5 c-d).

3.2 A monthly tidal envelope factor (F_M^S) for semi-diurnal regimes

The four types of monthly tidal envelope types found around ANZ are essentially different combinations of spring-neap and perigean-apogean signals. Thus, in a similar manner to van der Stok's (1897) method for calculating *daily* tidal form factors, a *monthly* tidal envelope factor (F_M^S) may be calculated for semi-diurnal tidal regions, including that of ANZ, according to:

$$F_M^S = \frac{a_{\mathrm{M}_2}+a_{\mathrm{N}_2}}{a_{\mathrm{M}_2}+a_{\mathrm{S}_2}}, \quad (1)$$

which can be further expressed as:

$$F_M^S = \frac{1+\frac{a_{\mathrm{S}_2}}{a_{\mathrm{M}_2}}x}{1+\frac{a_{\mathrm{S}_2}}{a_{\mathrm{M}_2}}}, \text{ with } x = \frac{a_{\mathrm{N}_2}}{a_{\mathrm{S}_2}} \quad (1a)$$

for areas characterized by more stable (e.g., lower variability) values of $\frac{a_{\mathrm{S}_2}}{a_{\mathrm{M}_2}}$ compared to $\frac{a_{\mathrm{N}_2}}{a_{\mathrm{S}_2}}$, or as:

$$F_M^S = \frac{1+\frac{a_{\mathrm{N}_2}}{a_{\mathrm{M}_2}}}{1+\frac{a_{\mathrm{N}_2}}{a_{\mathrm{M}_2}}y}, \text{ with } y = \frac{a_{\mathrm{S}_2}}{a_{\mathrm{N}_2}} \quad (1b)$$

for areas characterized by more stable (e.g., lower variability) values of $\frac{a_{\mathrm{N}_2}}{a_{\mathrm{M}_2}}$ compared to $\frac{a_{\mathrm{S}_2}}{a_{\mathrm{N}_2}}$.

https://doi.org/10.5194/os-2019-122
Preprint. Discussion started: 11 December 2019

Ocean Science Discussions

F_M^S takes into account the roles of the S_2 and N_2 tides in spring-neap and perigean-apogean cycles, while also factoring in the strong M_2 tide influence in both types of cycle. F_M^S may be used to classify the monthly tidal envelope types of any semi-diurnal region (i.e. where F<0.25) based on the analysis of constituent amplitudes and ratios from local data . Below we explain the four steps undertaken to successfully set the boundaries between different monthly tidal envelope types, thereby classifying the region's tides, using our ANZ case study data.

Step 1: Separating regimes dominated by spring-neap versus perigean-apogean signals

Fundamentally, in any semi-diurnal tidal regime (F<0.25) anywhere in the world where $\frac{a_{N_2}}{a_{S_2}} < 1$, spring-neap cycles will be a clear feature of the tidal height records (Table 1). This applies to the waters around ANZ. Thus, we set an initial boundary between different monthly tidal envelope types at $\frac{a_{N_2}}{a_{S_2}} = 1$ (Table 4). That is, regimes where $\frac{a_{N_2}}{a_{S_2}} < 1$ feature stronger spring-neap cycles, while regimes with $\frac{a_{N_2}}{a_{S_2}} > 1$ feature stronger perigean-apogean signals. As summarized in Table 2, compared to areas that experience stronger spring-neap influences, areas of the ANZ coast with stronger perigean-apogean influences are characterized by relatively smaller S_2 amplitudes (2-18 cm), with stronger N_2 amplitudes (10-22 cm).

Step 2: Separating regimes with consistent versus irregular and unequal spring-neap

Tidal regimes with stronger spring-neap signals (i.e. where $\frac{a_{N_2}}{a_{S_2}} <1$) include places where spring-neap cycles occur as consecutive fortnightly cycles of similar magnitude (hereafter labelled Type 1 or 'spring-neap' type regimes), and places where spring-neap signals dominate but with noticeable variability in the magnitudes of consecutive cycles due to subordinate perigean-apogean influences (hereafter labelled Type 2 or 'intermediate, spring-neap' regimes). In ANZ the strongest spring-neap influence occurs in the greater Cook Strait area, including at Kapiti where harmonic analysis revealed $\frac{a_{N_2}}{a_{S_2}} = 0.35$ (Table A1).

To set a boundary between Types 1 and 2 in any semi-diurnal tidal regimes around the world (and between Types 3 and 4 as explained below), it was necessary to take account of the moderating influence of the M_2 amplitude compared to the magnitudes of the S_2 and N_2 amplitudes, since the M_2 constituent influences monthly tidal envelopes at both synodic (spring-neap) and anomalistic (perigean-apogean) timescales (Table 1). In order to do this, experiments were conducted to explore two additional ratios:

i. the ratio of the 'annual' maximum tidal range to the subsequent tidal range (MTR); and
ii. the ratio of the 'annual' maximum spring tide range to the subsequent spring tide range (MSR).

We determined that the monthly tidal envelope boundary (F_M^S) between spring-neap (Type 1) and intermediate, spring-neap dominant (Type 2) regimes would occur at point where the MTR and MSR tidal range ratios exhibited the same value. 360 days of synthetic tidal range data were generated under conditions of F=0.25 (the boundary between 'semi-diurnal' and 'mixed, mainly semi-diurnal' type daily forms); and $a_{M_2} = 3a_{S_2}$; $a_{K_1} = a_{O_1}$; and $g_{M_2} = g_{S_1} = g_{K_1} = g_{O_1} = 0°$ (a subset of the assumptions employed by Courtier, 1938).When F=0.25, calculations revealed that the MTR value was 0.795. When the MSR ratio was set to the same value (0.795), calculations revealed that the F_M^S value was 0.795 (Figure A1). Based on this value, a review of our observation records revealed that the Kapiti site, with its F_M^S value of 0.79, exhibited the only completely spring-neap dominated site amongst our ANZ records. Hence we found that the boundary between monthly tidal envelope Types 1 and 2 in ANZ would site somewhere between the tidal regimes of Kapiti and the site with the next strongest spring-neap influence, Manukau, where $F_M^S = 0.93$.

https://doi.org/10.5194/os-2019-122
Preprint. Discussion started: 11 December 2019

Step 3: Separating regimes with 'perigean-apogean' and 'intermediate, perigean-apogean dominated' monthly tidal envelopes

Amongst our case study sites, areas with the most extreme perigean-apogean signal typically exhibited $\frac{a_{S_2}}{a_{M_2}}$ values of about 0.04 to 0.05 (Table A1). In order to determine the boundary between 'perigean-apogean' and 'intermediate, perigean-apogean dominant' regimes (i.e. Types 3 and 4), we conducted 31 experiments each generating 360 days of synthetic tidal ranges based on the fixed condition of $\frac{a_{S_2}}{a_{M_2}} = 0.05$, but with $\frac{a_{N_2}}{a_{S_2}}$ values ranging from 3 to 6 at intervals of 0.01 using Eq. (1a). Examining the shapes of the resultant monthly tidal envelopes, we were able to set a boundary value between Types 3 and 4 regimes at $F_M^S = 1.15$ in NZ waters (Table 4, Figure 6).

In summary, Figure 7 illustrates the classification of monthly tidal envelope types in the waters around ANZ using F_M^S. We find the west coast is characterized by Type 2 monthly tidal envelopes, with two unequal spring-neap cycles per month. Type 1 monthly tidal envelopes, with their defined spring-neap tides, are only found in the Cook Strait area. This area's defined spring-neap tides were explored in detail by Walters et al. (2010) - Figure 6 includes a re-analysis of their data using the F_M^S ratios. In contrast, the central east coast shows Type 4, perigean-apogean tidal envelopes, which is unusual for semi-diurnal regimes internationally (i.e. Figure 1c). Type 3 or intermediate, perigean-apogean dominated monthly tidal envelopes are found in the rest of the waters surrounding ANZ.

4 Discussion and conclusion

Daily tidal water level variations are a key control on shore ecology; access to marine environments via boat and shipping infrastructure such as ports, jetties and wharves; drainage links between the ocean and coastal hydrosystems such as lagoons and estuaries; and the duration and frequency of opportunities to access the intertidal zone for recreation and food harvesting purposes. Fortnightly and monthly tidal envelope variations, such as those associated with spring-neap and perigean-apogean cycles, have similar moderating roles on human usage of intertidal and shoreline environments, and additionally these medium term variations in tide levels are important factors in coastal inundation risks (Menéndez & Woodworth, 2010; Stephens 2015; Stephens et al., 2014; Wood, 1978, 1986;). High perigean-spring tides, for example, interact with extreme weather events (including low pressures, strong winds and extreme rainfall) to produce significant coastal inundation in low-lying coastal settlements such as on deltas (Hart et al., 2015).

In a world of rising sea levels, and coastal inundation hazard cascades (Menéndez and Woodworth, 2010), having common ways of describing different types of tidal envelope is essential for living safely and productively in coastal cities. This paper has employed observations from ANZ, FES2014 tidal data, and theoretical experiments, to demonstrate a simple approach to classifying different monthly tidal envelope types, applicable to semi-diurnal regions anywhere. The result is a widely applicable monthly tidal envelope factor (F_M^S) for classifying semi-diurnal regimes based on the amplitudes and amplitude ratios of three key constituents operating at synodic anomalistic timescales (M_2, S_2, and N_2).

At a very basic level, in any semi-diurnal tidal regime anywhere in the world where the value of $\frac{a_{N_2}}{a_{S_2}} < 1$, then spring-neap cycles will be clearly visible in tidal height records, either as consecutive fortnightly cycles of similar magnitude (Type 1), or as a dominant signal with noticeable variability in the magnitudes of consecutive fortnightly cycles, due to a subordinate perigean-apogean influence (Type 2). Conversely, in semi-diurnal areas of the world's oceans where $\frac{a_{N_2}}{a_{S_2}} > 1$, then perigean-apogean cycles will be clearly visible, either as singularly evident monthly cycles (Type 4), or as a dominant influence with subordinate spring-neap signals (Type 3). As illustrated in Sect. 3.2, quantitatively determining the actual boundaries between monthly tidal envelope Types 1 versus 2, and Types 3 versus 4 regimes at a local scale involves analysis of observational data, taking into account the moderating influence of the M_2 amplitude compared to the magnitudes of the S_2 and N_2 amplitudes.

https://doi.org/10.5194/os-2019-122
Preprint. Discussion started: 11 December 2019

Figure 1b illustrates the division of the semi-diurnal areas of the world's oceans into those where spring-neap cycles are the main monthly tidal envelope influence versus those where the perigean-apogean signal is paramount, while Figure 1c illustrates areas of the world's oceans where spring-neap signals are minor compared to 'perigean-apogean' influences in the monthly tidal envelope. The potentially predictable but relatively lower frequency tidal water level fluctuations such as those in our perigean-apogean monthly envelope classes are an important cause and moderator of coastal inundation hazards in different locations around the world (e.g. Wood 1978, 1986; Stephens 2015).

The simple approach to classifying monthly tidal envelope types in semi-diurnal regions demonstrated in this paper complements the existing, commonly used way of describing daily tidal forms based on the amplitudes of the four key, diurnal (K_1, O_1) and semi-diurnal (M_2, S_2) constituents (e.g. Defant 1958). We hope that our work inspires other efforts to study tidal height variations at timescales greater than daily, work which could draw renewed attention to the fundamental role of tidal water levels in shaping coastal environments, including in hazards such as low-frequency coastal flooding.

Data Availability

The tidal data used in this paper are available from LINZ (2017a; 2017b), NIWA (2017) and Walters et al. (2010). Details of the FES2014 tide model database are found in Carrere et al. (2016) and via https://www.aviso.altimetry.fr/en/data/products/auxiliary-products/global-tide-fes.html). Appendix 1 contains the data produced from analysis of these primary resources in this paper.

https://doi.org/10.5194/os-2019-122
Preprint. Discussion started: 11 December 2019

Ocean Science Discussions
Open Access

Appendix 1

Table A1. Values for 5 tidal harmonic constants, tidal ranges, form factors (*F*), and monthly tidal envelope factor (F_M^S) for a semi-diurnal regime used in classifying tidal envelope forms, for 23 stations around New Zealand, and compared to values derived from Equilibrium Theory

Station name (record used)	M_2		S_2		N_2		K_1		O_1		F	F_M^S	Type
	a_i (cm)	g_i (deg.)	a_i (cm)	g_i (deg.)	a_i (cm)	g_i (deg.)	a_i (cm)	g_i (deg.)	a_i (cm)	g_i (deg.)			
Equilibrium Theory	-	-	-	-	-	-	-	-	-	-	0.68	-	-
Kapiti (2011)	55	280	26	336	9	277	2	195	2	18	0.05	0.790	1
Manukau (2011)	109	297	29	332	20	287	6	17	1	287	0.05	0.935	2
Westport (2015)	113	309	29	348	23	287	2	198	3	40	0.04	0.958	2
Charleston (2015.7.-2016.1)	106	319	27	344	22	304	3	6	3	243	0.05	0.962	2
Puysegur Point (2012)	78	350	19	13	17	335	3	316	4	245	0.07	0.979	2
North Cape (2010)	80	230	15	279	16	209	8	10	2	351	0.11	1.011	3
Boat Cove, Rauol Island (2012)	50	208	9	287	10	176	5	43	3	44	0.14	1.017	3
Dog Island (2011)	91	33	18	57	21	6	2	119	4	60	0.06	1.028	3
Auckland (2011)	112	216	17	275	22	192	7	356	2	324	0.07	1.039	3
Fishing Rock, Raoul Island (2011)	52	206	8	283	11	178	5	35	2	41	0.12	1.050	3
Lottin Point (2011)	70	195	9	262	14	168	6	352	2	328	0.1	1.063	3
Tauranga (2011)	70	211	9	277	14	186	5	360	1	330	0.08	1.063	3
Korotiti Bay (2011)	78	207	11	265	16	181	6	349	1	317	0.08	1.056	3
Moturiki (2011)	73	189	10	265	15	156	5	173	1	136	0.07	1.060	3
Green Island (2011)	73	81	10	91	17	50	3	93	4	44	0.08	1.084	3
Port Chalmers (2011)	77	112	9	112	17	89	3	270	3	247	0.07	1.093	3
Sumner (2011)	84	136	6	151	18	109	5	273	3	245	0.09	1.133	3
Gisborne (2010)	64	176	5	251	14	148	4	336	1	275	0.07	1.130	3
Napier (2011)	64	167	4	240	14	138	3	298	2	221	0.07	1.147	3
Kaikoura (2011)	65	146	3	171	14	117	4	275	4	233	0.12	1.162	4
Owenga, Chatham Island (2011)	48	149	2	224	10	119	2	246	2	179	0.08	1.160	4
Castlepoint (2011)	63	159	3	225	14	129	3	280	3	219	0.09	1.167	4
Wellington (2011)	49	148	2	352	11	116	2	268	3	219	0.1	1.176	4
Overall range	48-113	33-350	2-29	13-352	9-23	6-335	2-8	6-360	1-4	40-351	0.04-0.14	0.79-1.176	1-4

https://doi.org/10.5194/os-2019-122
Preprint. Discussion started: 11 December 2019

Ocean Science Discussions

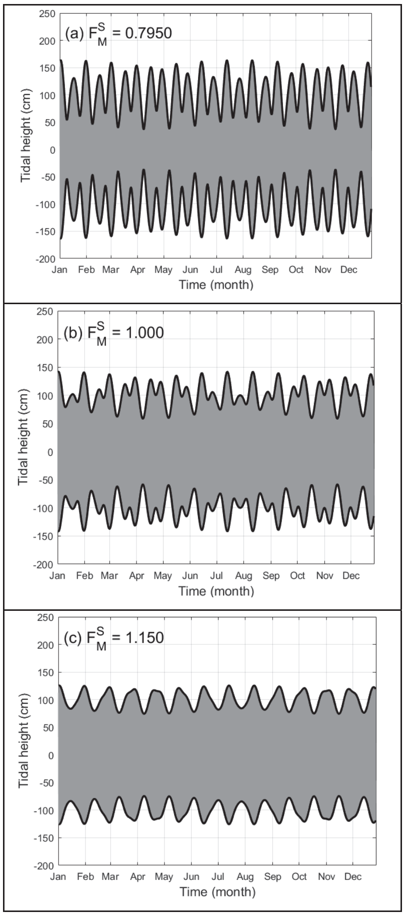

247 **Figure A1. Monthly tidal forms at the boundaries of the (a) '*spring-neap*' versus '*intermediate, spring-neap dominant*' tidal forms; at**
248 **the (b) '*intermediate, spring-neap dominant*' versus '*intermediate, perigean-apogean dominant*' tidal forms; and at the (c)**
249 **'*intermediate, perigean-apogean dominant*' versus '*perigean-apogean'* tidal forms, produced using the conditions summarized in**
250 **Table A1.**

251

https://doi.org/10.5194/os-2019-122
Preprint. Discussion started: 11 December 2019

Author contribution

Both authors conceived of the idea behind this paper. DH produced the initial manuscript draft. D-SB analyzed the tidal data and wrote the results sections. Both authors worked on and finalized the full manuscript.

Competing interests

The authors declare that they have no conflict of interest.

Acknowledgements

We are grateful to Land Information New Zealand (LINZ) and the National Institute of Water and Atmospheric Research (NIWA) for supplying the tidal data used in this research. Thank you to the University of Canterbury Erskine Programme for supporting D.-S. Byun during his time in New Zealand; to John Thyne for supplying Figure 2 map layers, and to Dr Derek Goring for interesting discussions regarding tidal data sources.

References

Andersen, O. B.: Global ocean tides from ERS 1 and TOPEX/POSEIDON altimetry, J. Geophys. Res., 100(C12), 25249, doi:10.1029/95JC01389, 1995.

Byun, D.-S. and Hart, D. E.: Predicting tidal heights for new locations using 25h of in situ sea level observations plus reference site records: A complete tidal species modulation with tidal constant corrections, J. Atmos. Ocean. Tech., 32, 350-371, 2015.

Carrere L., Lyard, F., Cancet, M., Guillot, A. and Picot, N.: FES 2014, a new tidal model - validation results and perspectives for improvements, Presentation to ESA Living Planet Conference, Prague, 2016.

Cartwright, D. E.: Tides: A scientific history, Cambridge; Cambridge University Press, 1999.

Courtier, A.: Marées. Service Hydrographique de la Marine, Paris, 1938.

D'Onofrio, E. E., Fiore, M. M., and Romero, S. I.: Return periods of extreme water levels estimated for some vulnerable areas of Buenos Aires, Cont. Shelf Res., 19(13), 1681-1693, 1999.

Defant, A.: Ebb and flow: the tides of earth, air, and water, Ann Arbor, University of Michigan Press, 1958.

Egbert, G. D., Bennett, A. F., and Foreman, M. G. G.: TOPEX/POSEIDON tides estimated using a global inverse model, J. Geophys. Res., 99(C12), 24821, doi:10.1029/94JC01894, 1994.

Hart D. E., Byun D.-S., Giovinazzi S., Hughes M. W. and Gomez C.: Relative Sea Level Changes on a Seismically Active Urban Coast: Observations from Laboratory Christchurch, Auckland, New Zealand, Proceedings of the Australasian Coasts and Ports Conference 2015, 15-18 Sep 2015, 6 pp., 2015.

Heath, R. A.: Phase distribution of tidal constituents around New Zealand, New Zeal. J. Mar. Fresh., 11(2), 383-392, 1977.

Heath, R. A.: A review of the physical oceanography of the seas around New Zealand—1982, New Zeal. J. Mar. Fresh., 19(1), 79-124, 1985.

LINZ, Land Information New Zealand: Sea level data downloads, http://www.linz.govt.nz/sea/tides/sea-level-data/sea-level-data-downloads, last access 2017a.

LINZ, Land Information New Zealand: Tides around New Zealand, https://www.linz.govt.nz/sea/tides/introduction-tides/tides-around-new-zealand, last access 2017b.

https://doi.org/10.5194/os-2019-122
Preprint. Discussion started: 11 December 2019

Masselink, G., Hughes, M., and Knight, J.: Introduction to Coastal Processes and Geomorphology (2 edn), Routeldge, 432 pp., 2014.

Menéndez, M., and Woodworth, P. L.: Changes in extreme high water levels based on a quasi-global tide-gauge data set, J. Geophys. Res., 115(C10) doi:10.1029/2009JC005997, 2010.

Nicholls, R. J., Wong, P. P., Burkett, V. R., Codignotto, J., Hay, J., McLean, R., Ragoonaden, S., Woodroffe, C. D., Abuodha, P. A. O., Arblaster, J. and Brown, B.: Coastal systems and low-lying areas, in: Parry, M. L., Canziani, O. F., Palutikof, J. P., van der Linden, P. J. and Hanson, C. E. (ed) Climate change 2007: impacts, adaptation and vulnerability, Contribution of Working Group II to the fourth assessment report of the Intergovernmental Panel on Climate Change, Cambridge, UK, Cambridge University Press, 315-356, 2007.

NIWA, National Institute of Water and Atmospheric Research: Sea level gauge records (hourly interval), https://www.niwa.co.nz/our-services/online-services/sea-levels, last access 2017.

Olson, D.-W.: Perigean spring tides and apogean neap tides in history, American Astronomical Society Meeting Abstracts, 219, 115.03, 2012.

Pawlowicz, R., Beardsley, B., and Lentz, S.: Classical tidal harmonic analysis including error estimates in MATLAB using T_TIDE, Comput. Geosci., 28(8), 929-937, doi:10.1016/S0098-3004(02)00013-4, 2002.

Pugh, D., and Woodworth, P.: Sea-level science: Understanding tides, surges, tsunamis and mean sea-level changes, Cambridge University Press, 394 pp., 2014.

Pugh, D. T.: Tides, surges and mean sea-level (reprinted with corrections), Chischester, U.K.; John Wiley & Sons Ltd, 486 pp., 1996.

Stammer, D., Ray, R. D., Andersen, O. B., Arbic, B. K., Bosch, W., Carrère, L., Cheng, Y., Chinn, D. S., Dushaw, B. D., Egbert, G. D. and Erofeeva, S. Y.: Accuracy assessment of global barotropic ocean tide models, Rev. Geophys., 52(3), 243-282, doi:10.1002/2014RG000450, 2014.

Stephens, S.: The effect of sea level rise on the frequency of extreme sea levels in New Zealand, NIWA Client Report No. HAM2015-090, prepared for the Parliamentary Commissioner for the Environment PCE15201, Hamilton, 52 pp., 2015.

Stephens, S. A., Bell, R. G., Ramsay, D., and Goodhue, N.: High-water alerts from coinciding high astronomical tide and high mean sea level anomaly in the Pacific islands region, J. Atmos. Ocean. Tech., 31(12), 2829-2843, 2014.

van der Stok, J. P.: Wind and water, currents, tides and tidal streams in the East Indian Archipelago. Batavia, 1897.

Walters, R. A., Gillibrand, P. A., Bell, R. G., and Lane, E. M.: A study of tides and currents in Cook Strait, New Zealand, Ocean Dynam., 60(6), 1559-1580, doi:10.1007/s10236-010-0353-8, 2010.

Walters, R. A., Goring, D. G., and Bell, R. G.: Ocean tides around New Zealand, New Zeal. J. Mar. Fresh., 35(3), 567-579, 2001.

Wood, F. J.: The strategic role of perigean spring tides in nautical history and North American coastal flooding, 1635-1976, Department of Commerce, 1978.

Wood, F. J.: Tidal dynamics: Coastal flooding and cycles of gravitational force, M.A., USA, D. Reidel Publishing Co., Hingham, 1986.

https://doi.org/10.5194/os-2019-122
Preprint. Discussion started: 11 December 2019

Ocean Science
Discussions
Open Access

Table 1. Tidal constituent pairs associated with different monthly tidal envelope contributors and their intervals, including their cycle types and controlling factors

Constituent pairs	Interval (days)	Cycle type	Control
M_2, S_2	14.7653	spring-neap	Moon phase, i.e. the axial alignment of Moon and Sun relative to Earth during the synodic month.
M_2, N_2	27.5546	perigean-apogean	Relative distance between the Moon and Earth throughout the Moon’s orbit over the anomalistic month.
K_1, O_1	13.6608	tropic-equatorial	Changes in the Moon’s declination during the sidereal month.

***Note*. With monthly tidal envelope characterization, the N_2 is considered in addition to the constituents included in daily tidal form classification (e.g. Defant 1958).**

https://doi.org/10.5194/os-2019-122
Preprint. Discussion started: 11 December 2019

Table 2. Comparison of tidal constituent amplitudes, amplitude ratios (including daily tidal form factor, *F*, and monthly tidal envelope factor, F_M^S) and ranges between the four distinct types of monthly tidal envelope found in the 23 case study semi-diurnal tide regimes of Aotearoa New Zealand, and compared to Equilibrium Theory amplitude ratios

Monthly tidal envelope description	$F\left(=\frac{K_1+O_1}{M_2+S_2}\right)$	Amplitudes (cm) of:					Amplitude ratios of:							Example sites
		M_2	S_2	N_2	K_1	O_1	$\frac{S_2}{M_2}$	$\frac{N_2}{M_2}$	$\frac{S_2}{N_2}$	$\frac{S_2+N_2}{M_2}$	$F_M^S\left(=\frac{M_2+N_2}{M_2+S_2}\right)$	$\frac{K_1}{M_2}$	$\frac{O_1}{M_2}$	
n/a	0.68 mixed diurnal	-	-	-	-	-	0.47	0.19	2.44	0.66	-	0.584	0.415	Equilibrium Theory*
Spring-neap type	0.05 semi-diurnal	55	26	9	2	2	0.47	0.16	2.89	0.64	0.79	0.04	0.04	Kapiti
Intermediate, spring-neap dominant	0.04 to 0.07 semi-diurnal	78 to 113	19 to 29	17 to 23	2 to 6	1 to 4	0.24 to 0.27	0.18 to 0.22	1.12 to 1.45	0.45 to 0.46	0.93 to 0.98	0.02 to 0.06	0.01 to 0.05	Manukau, Westport, Charleston, Pusegur Point
Intermediate, perigean-apogean dominant	0.06 to 0.14 semi-diurnal	50 to 112	4 to 18	10 to 22	2 to 8	1 to 4	0.06 to 0.2	0.2 to 0.23	0.29 to 0.94	0.28 to 0.43	1.01 to 1.15	0.02 to 0.10	0.01 to 0.06	North Cape, Boat Cove and Fishing Rock (Raoul Island), Dog Island, Auckland, Lottin Point, Tauranga, Korotiti Bay, Moturiki, Green Island, Port Chalmers, Sumner, Gisborne, Napier
Perigean-apogean type	0.08 to 0.12 semi-diurnal	48 to 65	2 to 3	10 to 14	2 to 4	2 to 4	0.04 to 0.05	0.21 to 0.22	0.18 to 0.21	0.25 to 0.27	1.16 to 1.18	0.04 to 0.06	0.04 to 0.06	Kaikoura, Owenga, Castlepoint, Wellington

***Note*. Data sourced from this research, and from Defant (1958)* (for tidal station details, including tidal phase-lags, see Appendix 1 Table A1).**

https://doi.org/10.5194/os-2019-122
Preprint. Discussion started: 11 December 2019

Ocean Science
Discussions
Open Access

Table 3. Monthly tidal envelope factor (F_M^S) for classifying different monthly tidal types in Aotearoa New Zealand's semi-diurnal tidal regime

F_M^S	Type	Name	Description of monthly tidal envelope
< 0.795	1	Spring-neap type	Two similar magnitude spring-neap cycles.
> 0.795 *and* < 1.0	2	Intermediate, spring-neap dominated	Two unequal spring-neap cycles.
> 1.0 *and* < 1.15	3	Intermediate, perigean-apogean dominated	A strong perigean-apogean cycle plus two weaker spring-neap cycles.
> 1.15	4	Pperigean-apogean type	A distinct perigean-apogean cycle.

https://doi.org/10.5194/os-2019-122
Preprint. Discussion started: 11 December 2019

Ocean Science
Discussions

Table 4. Typical (representative) input and boundary values for classifying monthly tidal envelope types around the Aotearoa New Zealand coast

F_M^S boundary case	Eq. (1)		F_M^S	Notes
	Given value	x or y		
Type 1 vs. Type 2	$\frac{a_{S_2}}{a_{M_2}} = 0.47$	$x = 0.36$	0.8	When MSR≈MTR with F=0.25, then the value of F_M^S; $a_{S_2} = 2.78\, a_{N_2}$
Type 2 vs. Type 3	$\frac{a_{N_2}}{a_{M_2}} = 0.21$	$y = 1$	1	$a_{S_2} = a_{N_2}$
Type 3 vs. Type 4	$\frac{a_{S_2}}{a_{M_2}} = 0.05$	$x = 4.024$	1.15	$a_{S_2} = 0.249\, a_{N_2}$

Note. **$x = \frac{a_{N_2}}{a_{S_2}}$ and $y = \frac{a_{S_2}}{a_{N_2}}$. MSR and MTR denote the ratio between the maximum spring tide range to the subsequent spring tide range and the ratio between the 'annual' maximum tidal range to the subsequent tidal range, respectively.**

https://doi.org/10.5194/os-2019-122
Preprint. Discussion started: 11 December 2019

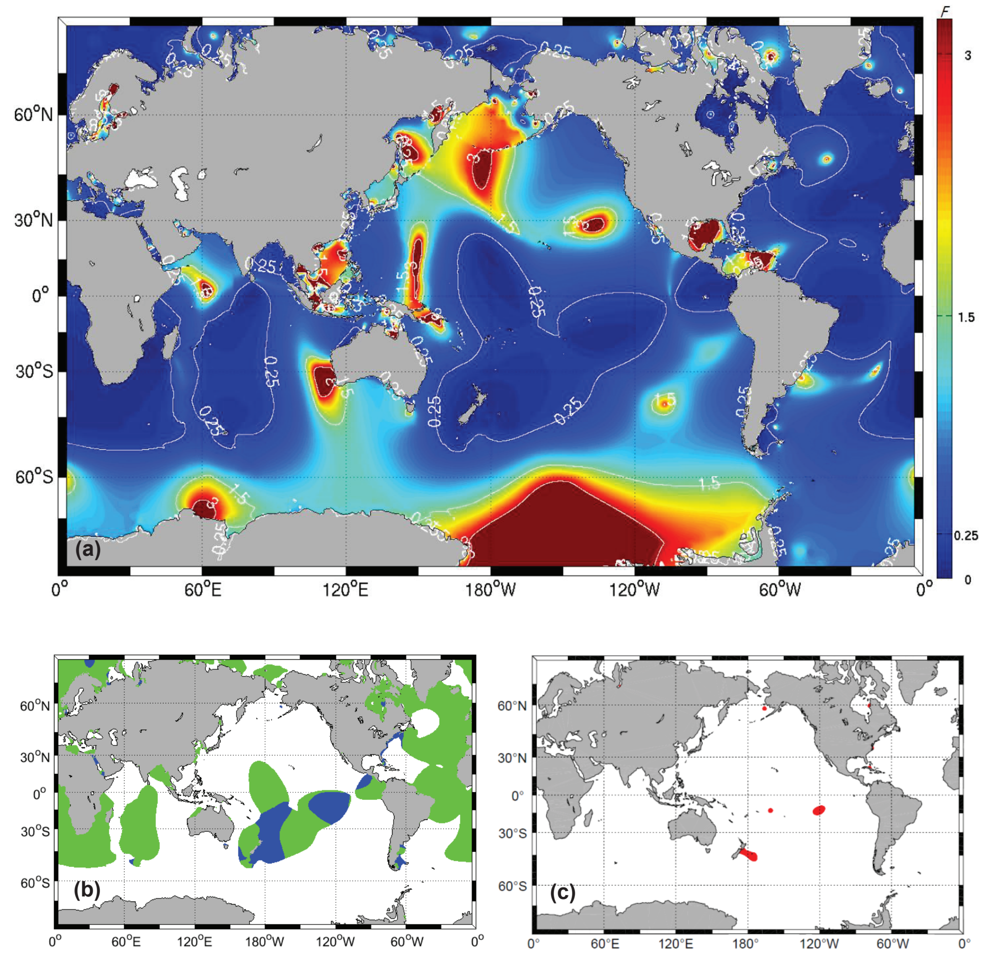

Figure 1. (a) Global distribution of daily form factor (*F*) values, indicating daily tidal regime types (*F*<0.25: semi-diurnal; *F*>0.25 to *F*<1.5 mixed-mainly semi-diurnal; *F*>1.5 to *F*<3: mixed-mainly diurnal; and *F*>3: diurnal, according to the classification of van der Stok 1897, and Courtier 1938); (b) the world's semi-diurnal tidal areas (*F*<0.25) divided into those where spring-neap (green) versus perigean-apogean (blue) signals are the main influence on the monthly tidal envelope; and (c) semi-diurnal tidal regimes (in red) where the S_2/M_2 constituent amplitude ratio is <0.04 and thus spring-neap tidal signals are very weak so that perigean-apogean signals are prominent, as derived from FES2014 tidal harmonic constants.

https://doi.org/10.5194/os-2019-122
Preprint. Discussion started: 11 December 2019

Ocean Science
Discussions
Open Access

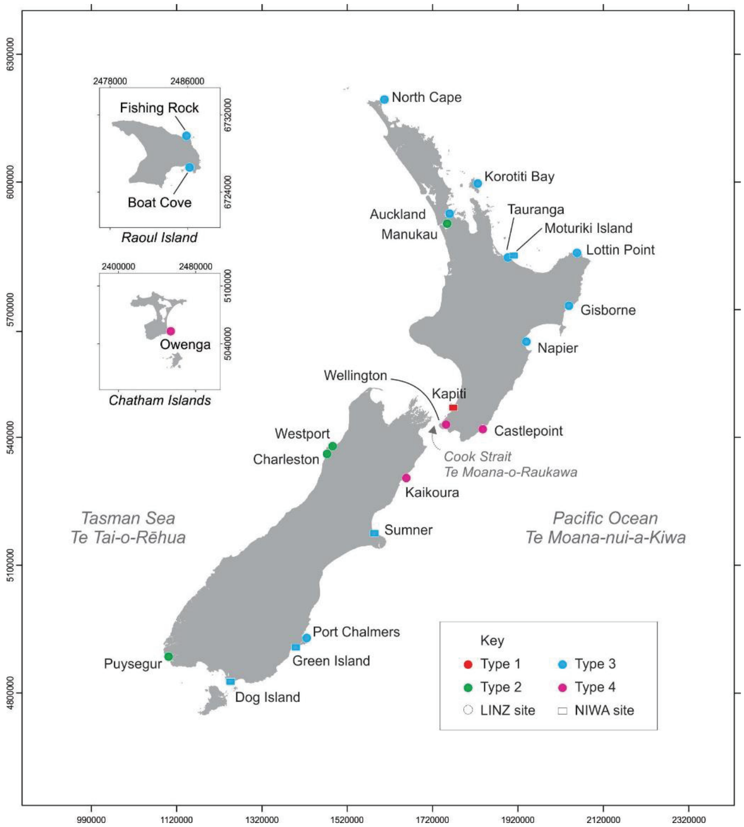

Figure 2. Location of 23 Aotearoa New Zealand sea level observation stations investigated in this research: circles indicate LINZ sites, rectangles indicate NIWA sites; each site is colored according to monthly tidal envelope type. Offshore islands are not shown to scale (Raoul & Chatham Islands). The coordinate system is NZGD2000, Transverse Mercator.

https://doi.org/10.5194/os-2019-122
Preprint. Discussion started: 11 December 2019

Ocean Science
Discussions
Open Access

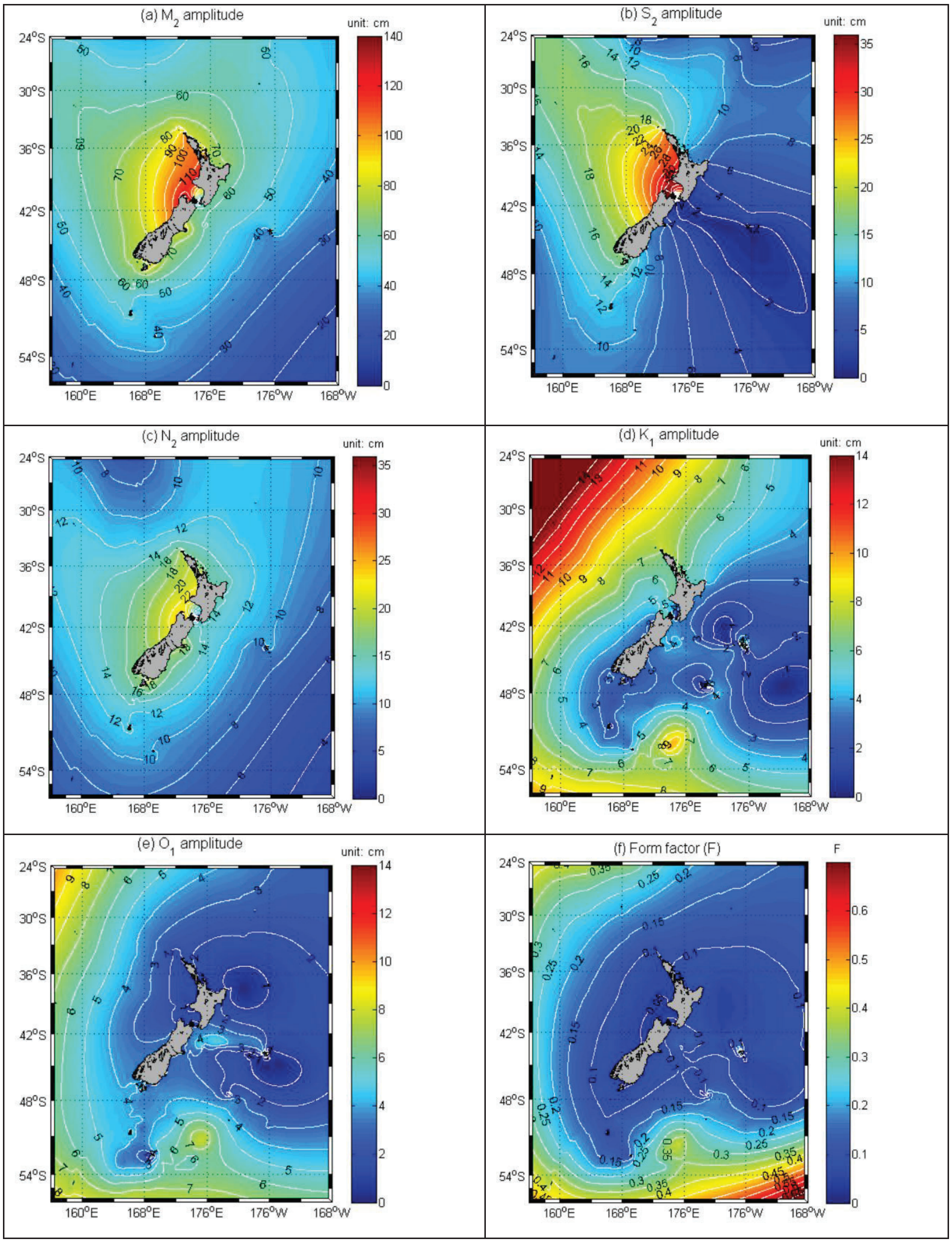

https://doi.org/10.5194/os-2019-122
Preprint. Discussion started: 11 December 2019

Figure 3. Amplitude contours for the (a) M_2, (b) S_2, (c) N_2, (d) K_1, and (e) O_1 tides around ANZ, and (f) the resultant horizontal distribution of *F*, daily tidal form factor values, as derived and calculated from the FES2014 tide model database at a scale of 1°/16×1°/16. Note that the amplitude color scales vary between plots a and e.

https://doi.org/10.5194/os-2019-122
Preprint. Discussion started: 11 December 2019

Ocean Science Discussions
Open Access
EGU

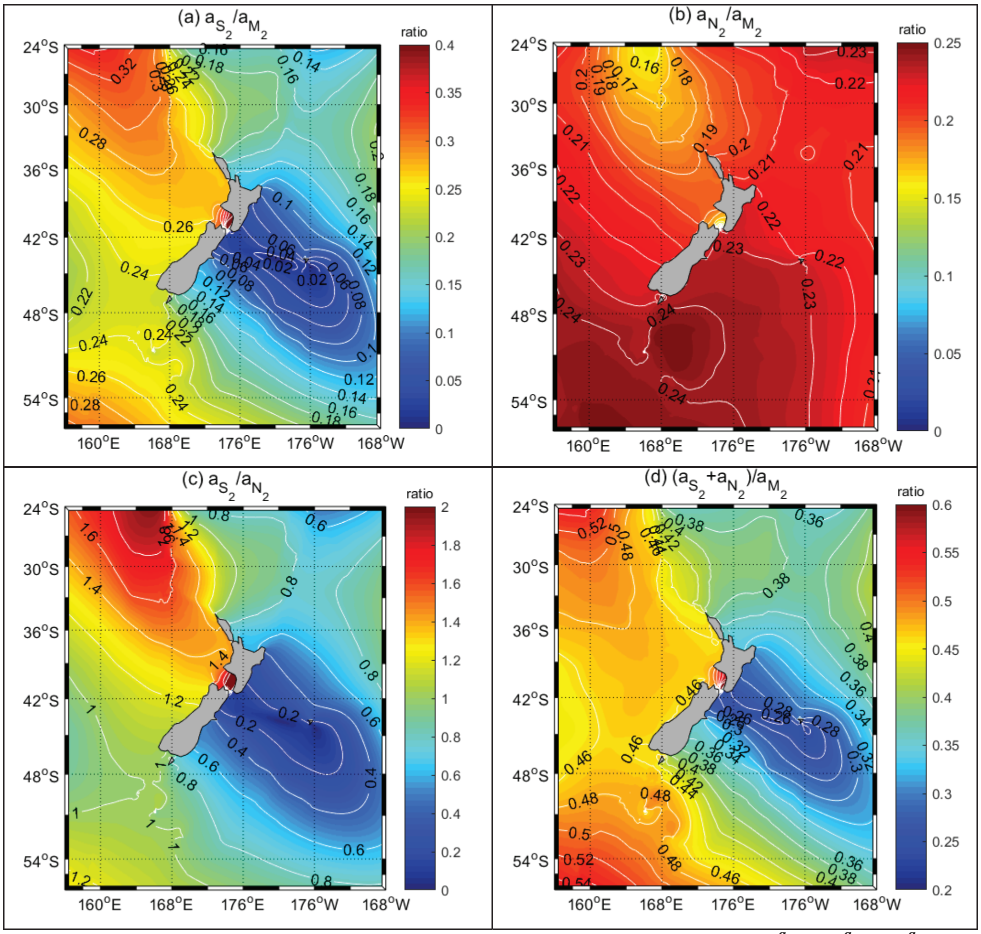

Figure 4. Horizontal distributions of tidal constituent amplitude ratios around ANZ for: (a) $\frac{a_{S_2}}{a_{M_2}}$; (b) $\frac{a_{N_2}}{a_{M_2}}$; (c) $\frac{a_{S_2}}{a_{N_2}}$ and (d) $\frac{a_{S_2+}a_{N_2}}{a_{M_2}}$; as calculated using the FES2014 tide model database at a scale of 1°/16×1°/16. Note that the amplitude color scales vary between plots a and d.

https://doi.org/10.5194/os-2019-122
Preprint. Discussion started: 11 December 2019

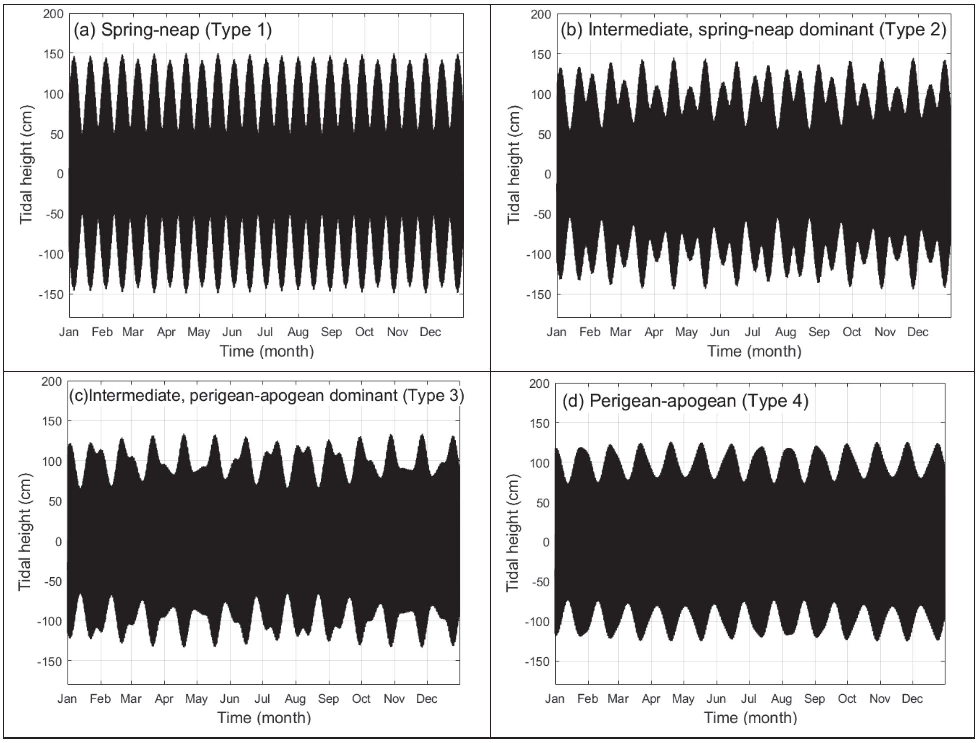

Figure 5. Idealized examples of four different monthly tidal envelopes over one year, calculated using the amplitude value $a_{M_2} = 100\ cm$ and the amplitude ratio values of: (a) $\frac{a_{S_2}}{a_{M_2}} = 0.46$, $\frac{a_{S_2}}{a_{N_2}} = 11.5$, $\frac{a_{N_2}}{a_{M_2}} = 0.04$; (b) $\frac{a_{S_2}}{a_{M_2}} = 0.27$, $\frac{a_{S_2}}{a_{N_2}} = 1.5$, $\frac{a_{N_2}}{a_{M_2}} = 0.18$; (c) $\frac{a_{S_2}}{a_{M_2}} = 0.12$, $\frac{a_{S_2}}{a_{N_2}} = 0.5455$, $\frac{a_{N_2}}{a_{M_2}} = 0.22$; and (d) $\frac{a_{S_2}}{a_{M_2}} = 0.04$, $\frac{a_{S_2}}{a_{N_2}} = 0.1818$, $\frac{a_{N_2}}{a_{M_2}} = 0.22$. Note that the F_M^S values of these plots are: (a) 0.71; (b) 0.93; (c) 1.09; and (d) 1.17.

https://doi.org/10.5194/os-2019-122
Preprint. Discussion started: 11 December 2019

Ocean Science
Discussions

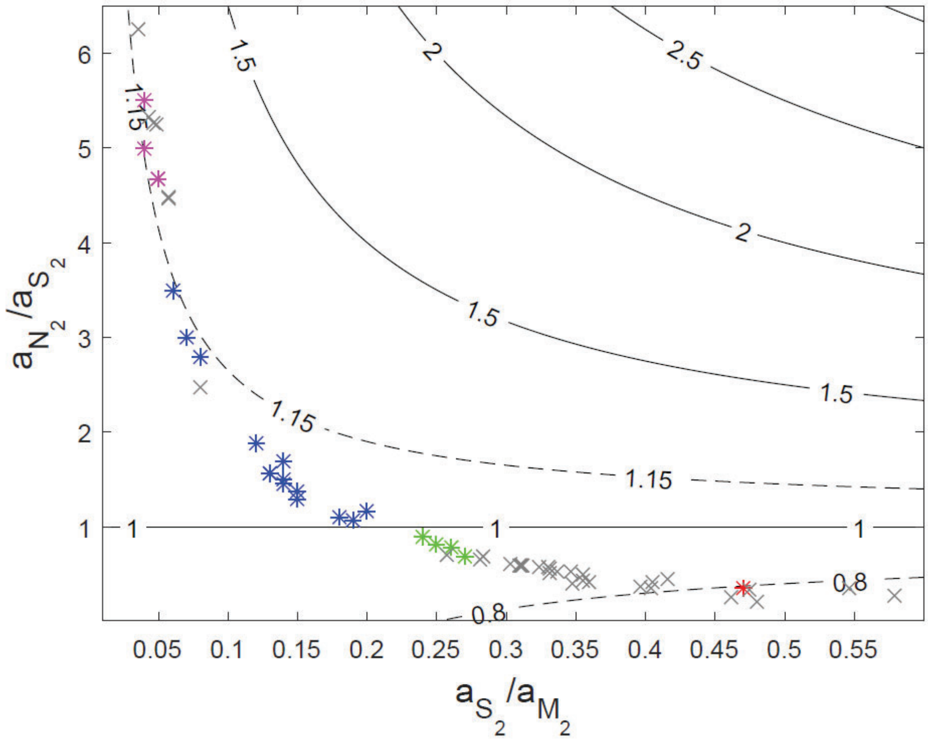

367

368 **Figure 6. Plot of the relationship between the $\frac{a_{N_2}}{a_{S_2}}$ and $\frac{a_{S_2}}{a_{M_2}}$ ratios (y and x axes respectively) versus F_M^S values (shown as plot contours),**
369 **with data points corresponding to Aotearoa New Zealand waters Type 1 sites (red star); Type 2 sites (green stars); Type 3 sites (blue**
370 **stars); and Type 4 sites (pink stars), all from Table 2; and tidal data representative of the greater Cook Strait area (grey crosses)**
371 **from Walters et al. (2010, Tables 1 and 3).**

372

https://doi.org/10.5194/os-2019-122
Preprint. Discussion started: 11 December 2019

Ocean Science
Discussions
Open Access

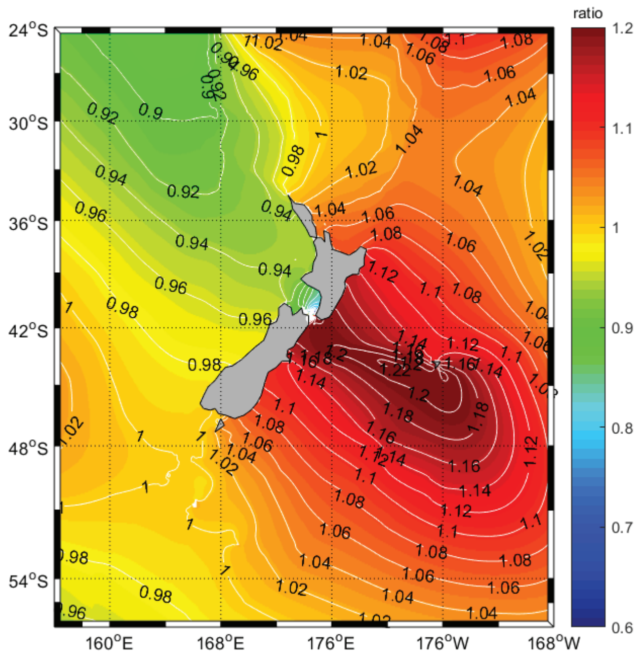

Figure 7. Distribution of monthly tidal envelope factor (F_M^S) values in the waters around ANZ, calculated using FES2014 data. See Table 3 and Figure 5 for corresponding monthly tidal envelope factor classes and envelope patterns.